Grain refinement in aluminum alloy 2219 during ECAP at 250 °C

I. Mazurina [a,*], T. Sakai [a], H. Miura [a], O. Sitdikov [b,c], R. Kaibyshev [b]

[a] *Department of Mechanical Engineering and Intelligent Systems, UEC Tokyo (The University of Electro-Communications), Chofu, Tokyo 182-8585, Japan*

[b] *Institute for Metals Superplasticity Problems, Khalturina 39, Ufa 4500001, Russia*

[c] *Department of Engineering Physics, Electronics and Technology, Nagoya Institute of Technology, Nagoya 466-8555, Japan*

Abstract

Grain refinement taking place in a coarse grained 2219 aluminum alloy deformed by equal channel angular pressing (ECAP) at a temperature of 250 °C to a strain of 12 was investigated. The microstructural changes are mainly characterized by the evolution of high density dislocation substructures with relatively low misorientations (~3–5°) at strains below 2 and deformation bands (DBs) with moderate misorientation angle, which are frequently formed at strains above 3. Repeated ECAP leads to increasing the number and misorientation angle of the boundaries of DBs, so that the misorientation distribution for newly evolved dislocation subboundaries changes from single peak type at low strains to bimodal one at high strains. The fraction of high angle boundaries starts to increase at strain $\varepsilon = 3$, then it rapidly rises to about 80% at moderate to high strains and a new fine grains with almost random crystal orientation are fully developed in a whole material. The main mechanism of new fine grained structure formation during ECAP is discussed.

Keywords: Equal channel angular pressing (ECAP); Deformation band (DB); Grain fragmentation; Aluminum alloy 2219

1. Introduction

Equal channel angular pressing (ECAP) is one of the popular methods of severe plastic deformation, which is often used to produce ultrafine grained structure in metallic materials [1,2]. It is well known that ECAP can provide large amount of plastic deformation and results in several important effects on microstructure and properties of metals and alloys [1–5]. Most of the published papers deals with improvement of the mechanical properties of fine grained materials, while a few attempts to characterize microstructural changes and to discuss the mechanisms, which are responsible for the new grain formation during ECAP [5–9]. One of the main proposed mechanisms is continuous dynamic recrystallization (cDRX) frequently operating in a wide range of metallic materials including aluminum alloys during deformation at elevated and high temperatures [5–13]. It is originally associated with formation of low angle subgrain boundaries at early stages of deformation and their gradual transformation into high angle ones with further straining due to accumulation of lattice dislocations [1,11,12].

Hot deformation to a very large strain of high recovery metallic materials, such as Al and its alloys, can result into operation of another mechanism, associated with evolution of the initial grains. Simply put, severe deformation makes the original coarse grains thin down and, as result, strongly serrated boundaries eventually touch and pinching-off the grains into short lengths, which is regarded as geometric dynamic recrystallization [11–13]. However, it was pointed out [14] that during hot deformation, transformation of initial coarse grained structure to fine grained one occurs due to frequent operation of dynamic recovery and inhomogeneous grain boundary sliding, that is also known as cDRX. In addition, some recent papers [8,9,14–18] discussed that at the same deformation conditions mechanism of cDRX can be directly associated with grain fragmentation due to formation of geometrically necessary boundaries with persistent nature, such as microshear or kink bands, and their gradual increase in number and misorientation angle with severe plastic deformation. Thus, a satisfactory explanation of the mechanism of new grain formation is a subject of discussion.

* Corresponding author. Tel.: +81 424845404; fax: +81 424843327.
E-mail address: imazurina@yahoo.com (I. Mazurina).

The present study was carried out to examine the grain refinement process in a coarse grained 2219 aluminum alloy during ECAP at 250 °C. A special attention was paid to determining the origin of fine grained structure and the misorientation characteristics of deformation-induced boundaries. The operating structural mechanism is discussed in detail.

2. Experimental procedure

An aluminum alloy 2219 with a chemical composition of Al–6.4Cu–0.3Mn–0.18Cr–0.19Zr–0.06Fe (in mass%), as denoted herein AA2219, was manufactured at Kaiser Aluminum Center for Technology. The alloy was homogenized at 530 °C for 6 h as solution treatment and had an equiaxed grain structure with an average grain size ~140 μm. Samples for ECAP were machined parallel to the ingot axis into rods with a diameter of 20 mm and a length of 100 mm. ECAP was conducted at 250 °C using an isothermal die with a circular internal cross-section with a diameter of about 20 mm. The channel had an L-shaped configuration with an angle of intersection and that at the outer arc of curvature 90° both. Deformation through this channel produced a strain of about $\varepsilon = 1$ in each pass through the die [4]. The samples were pressed repeatedly up to strains of 12 at a temperature of 250 °C by using route A, i.e. without rotation of the billet in each pass. This route has been used in the author's previous works [9,18,19] and it is most effective for formation of fine grained structure with larger fraction of high angle boundaries (HABs) [7].

Each pressed sample was quenched in water after ECAP and finally cut parallel to the pressing direction in longitudinal section for microstructural observations. Metallographic analysis was carried out using an optical microscope (OM) after etching by the standard Dics-Keller etchant. The orientation imaging microscopy (OIM) with automated indexing of electron back scattering diffraction (EBSD) patterns was performed in Hitachi S-4300H scanning electron microscope (SEM) with OIM analysis software provided by TexSem Lab Inc. Thin discs with a diameter of 3 mm for transmission electron microscopy (TEM) examination were mechanically thinned and then electropolished in a solution of 30% HNO_3 and 70% CH_3OH at around −32 °C using a Tenupol-3 twin-jet polishing unit. Foils were examined using a JEOL-2000EX TEM. An average crystallite size and fraction recrystallized were measured by the linear intercept method. The misorientations of deformation-induced boundaries were measured using the conventional Kikuchi-line technique. A total number of boundaries analyzed were from 80 to 100 for each sample.

3. Experimental results

3.1. Optical microstructures

Typical optical microstructures developed during ECAP at 250 °C are shown in Fig. 1. ECAP results in elongation of initial grains and development of fibrous microstructures, which are aligned roughly parallel to the pressing direction (PD). At early stages of deformation ($\varepsilon = 1$–2), such fibrous structures are heterogeneously developed in some initial grain interiors due to formation of numerous deformation bands (DBs), which are indicated by arrow in Fig. 1(a). DBs increase in density with further deformation to moderate strain of $\varepsilon = 4$ (Fig. 1(b)). As a result, the substructural elements formed at this strain are distributed more homogeneously in the elongated grain interiors and the initial grain boundaries cannot be separated from these microstructures. The microstructures developed in high strain, however, cannot be examined in details by OM because of their complexity.

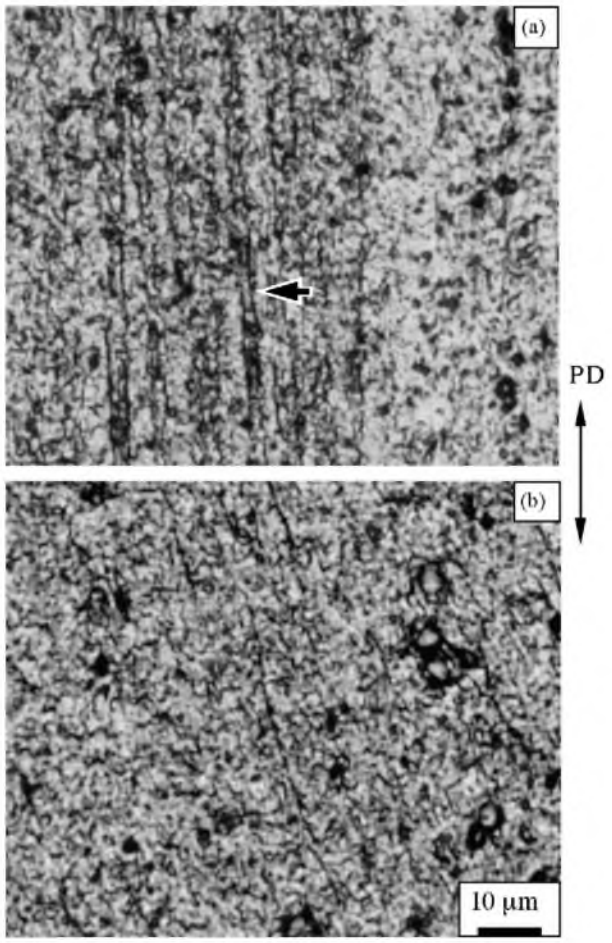

Fig. 1. Optical micrographs of 2219 Al alloy deformed by ECAP at 250 °C up to strains: (a) $\varepsilon = 2$ and (b) $\varepsilon = 4$. Arrow indicates deformation band (DB). PD is pressing direction.

3.2. OIM microstructures

Figs. 2–4 show typical OIM pictures in gray scale of the 2219 Al alloy deformed to various strains at 250 °C. In these OIM maps orientation differences ($\Delta\Theta$) between neighboring grid points, $\Theta \geq 2°$, $\Theta > 5°$ and $\Theta \geq 15°$ are marked by thin white, thin black and bold black lines, respectively. Here the point-to-point $\Delta\Theta$ and the cumulative $\sum\Delta\Theta$ misorientations developed along test line T_x are represented in each OIM figure. It is seen in Fig. 2(a) that ECAP at $\varepsilon = 1$ leads to the elongation of initial coarse grains. The substructures with low angle boundaries (LABs) less than 5° are homogeneously developed in interiors of

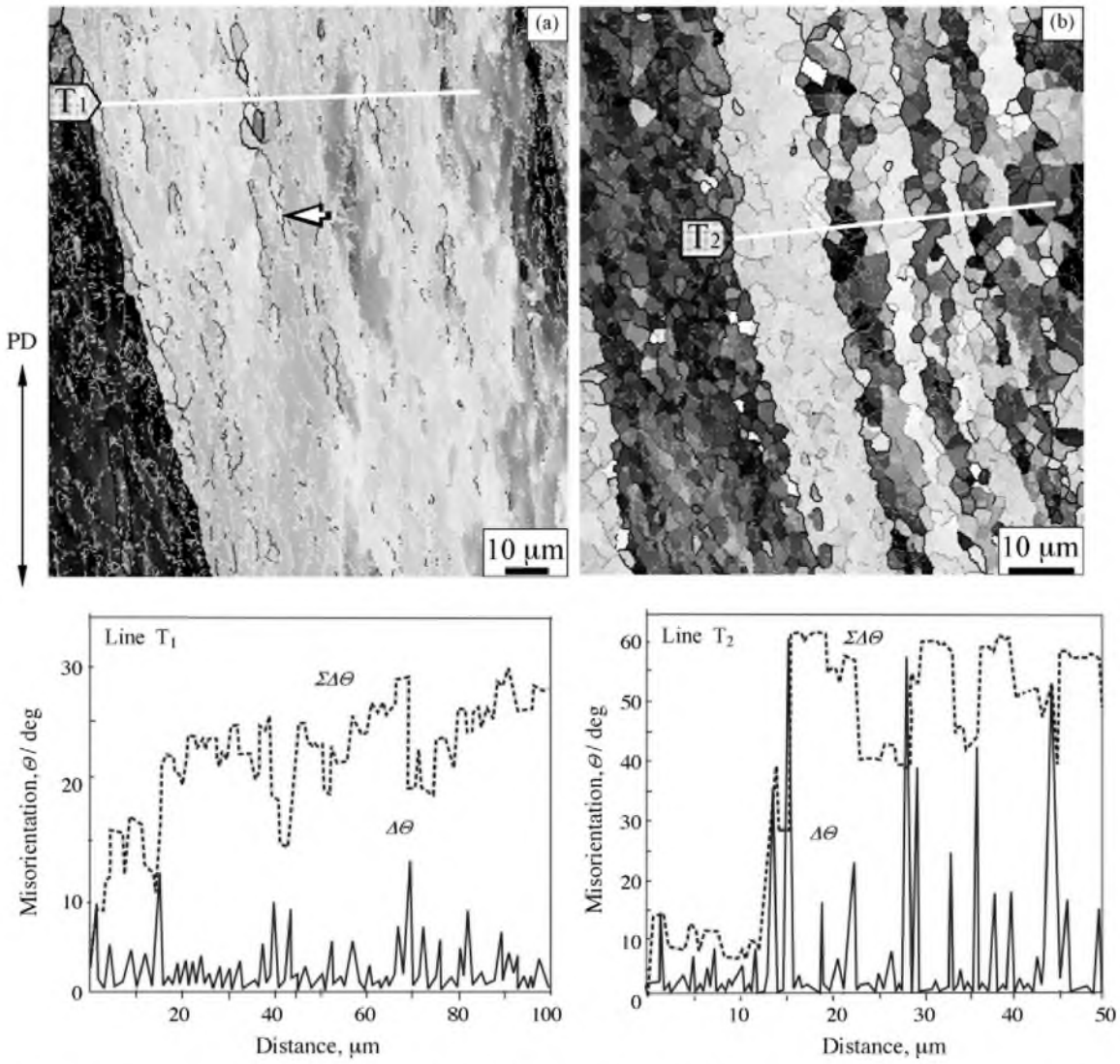

Fig. 2. OIM micrographs and corresponding misorientation profiles for 2219 Al alloy deformed by ECAP at 250 °C. Thin white lines correspond to the boundaries with misorientation $\Theta > 2^\circ$, thin black lines $\Theta > 5^\circ$ and bold lines $\Theta \geq 15^\circ$, respectively. (a) $\varepsilon = 1$; (b) $\varepsilon = 3$. Arrow indicates DB.

elongated grains accompanied by several boundaries with moderate angles from 5° to 10°. The latters, were observed roughly parallel to PD inhomogeniously distributed in the interiors, as shown by arrow in Fig. 2(a), and near original grain boundaries. They can be considered as embryos of DBs, which are frequently evolved at $\varepsilon > 2$. The other LABs correspond to those of conventional subgrains. The $\sum \Delta\Theta$ along T_1 tends to rise by increasing the distance from grain boundary accompanied by discontinuous changes at moderate angle boundaries of DBs. This suggests that significant orientation gradient is evolved in initial grains after one pass of ECAP. Further straining to $\varepsilon = 3$ leads to formation of fibrous microstructure due to increasing the number of DBs, as shown in Fig. 2(b). It is seen, that the misorientation angle distributed along line T_2 increased and the boundaries of DBs are corrugated with a length of fine subgrains surrounded mostly by moderate and high angle boundaries.

It should be noted, that deformed microstructure evolved at $\varepsilon = 3$ is inhomogeneous, and in some regions of grain interiors at the same strain, the fine (sub)grains are partially developed, as shown in Fig. 3(a). Misorientation distribution along line T_3 shows that these new (sub)grains are surrounded by boundaries with moderate to high angles, i.e. $15^\circ \leq \Theta \leq 50^\circ$ (Fig. 3(b)). The $\sum \Delta\Theta$ reveals frequent changes of lattice orientations separated by high angles with misorientation angles of above 15°, which correspond to the new grain boundaries. The crystal orientation of such fine (sub)grains developed at $\varepsilon = 3$ are randomized to some extent (Fig. 3(c)) in comparison with those in the other regions with fibrous microstructure in Fig. 2(b).

With further deformation to high strains $\varepsilon = 6$–12, the regions containing aligned microstructures, such as DBs, progressively decrease and those of new fine grains conversely increase. A typical OIM picture developed at $\varepsilon = 6$ is represented in Fig. 4(a). A microstructure consisting of new fine grains with high misorientation angles ranging from 15° to 60° is almost homogeneously developed in the whole area. It is remarkable to see that new evolved grains are not only equiaxed, but also elongated to the direction of PD. Note here also, that there are quite few remnant parts of original grains aligned to the PD, e.g. as indicated by

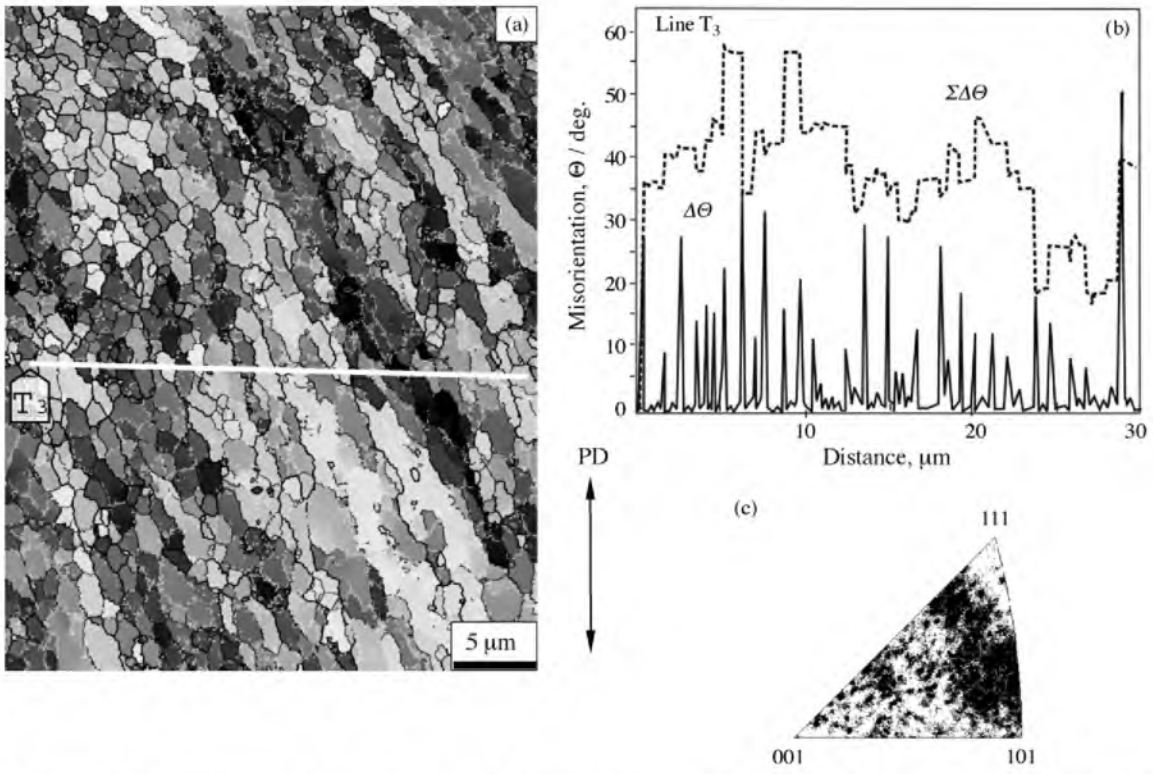

Fig. 3. (a) OIM micrograph, (b) the misorientation changes along line T_3, and (c) the inverse pole figure of 2219 Al alloy deformed by ECAP to $\varepsilon = 3$ at 250 °C.

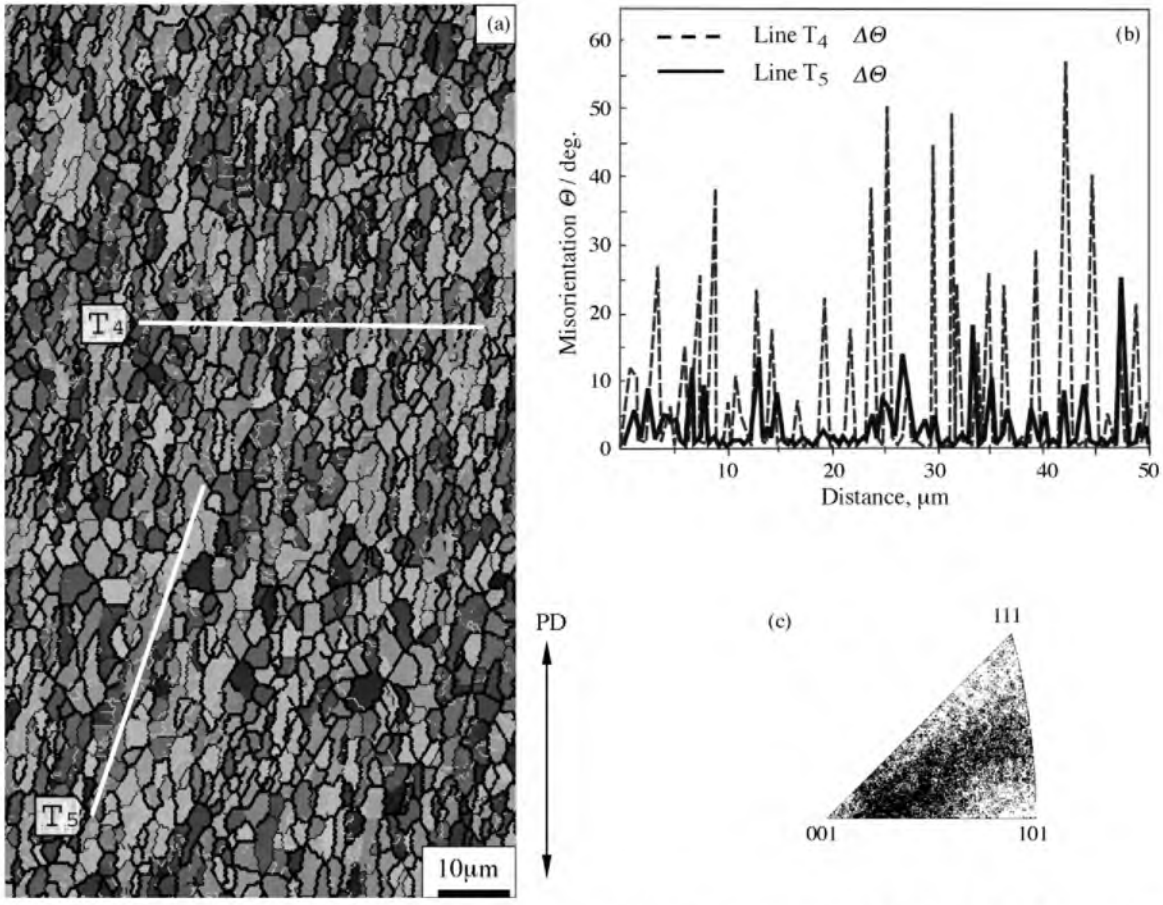

Fig. 4. (a) OIM micrograph and (b) the misorientation changes along lines T_4 and T_5 and (c) the inverse pole figure of the 2219 Al alloy deformed by ECAP to $\varepsilon = 6$ at 250 °C.

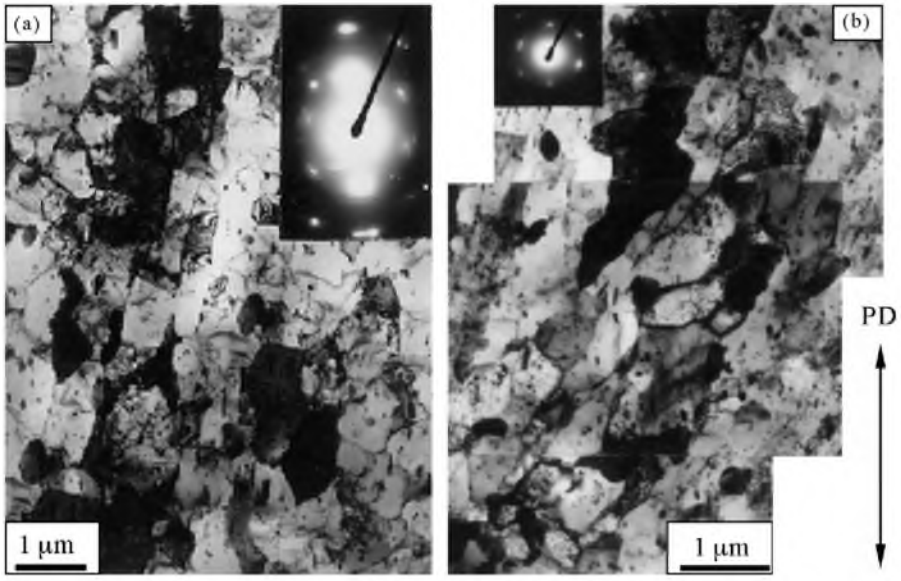

Fig. 5. TEM microstructures with diffraction patterns of 2219 Al alloy deformed by ECAP at 250 °C. (a) $\varepsilon = 2$ and (b) $\varepsilon = 4$.

solid line T_5 in Fig. 4(a). Dislocation subboundaries with low-to-moderate angle misorientations are mainly developed in such areas. The $\Delta\Theta$ changes along dashed line T_4 are much larger than those of T_5 (Fig. 4(b)) and correspond to the fine grained areas in Fig. 4(a). The inverse pole figure of Fig. 4(c) suggests, that further progress of randomization is taking place in such new grained regions formed during ECAP to strain of $\varepsilon = 6$ and higher.

3.3. TEM microstructures

Typical microstructures revealed by TEM at low and moderate strains are represented in Fig. 5. It can be seen that dislocation substructures with LABs are frequently formed in early stages of ECAP. Two types of subgrains can be observed at $\varepsilon = 1$ in Fig. 5(a). One of them consists of equiaxial subgrains with a size of about 1 μm and the misorientation angles of 2–4°, as it is suggested by a single spot diffraction pattern obtained from a selected area of 6 μm diameter. The other type is elongated subgrains evolved in localized regions which are roughly parallel to PD. Their length is two to three times larger than the transverse size of about 1.5 μm. Elongated subgrains may correspond to microstructures evolved in the interiors of DBs mentioned in Figs. 1 and 2. After subsequent deformation to moderate strain of $\varepsilon = 4$, the second type of substructure is more clearly developed in material and its fraction increased (Fig. 5(b)).

Typical TEM microstructures with misorientation maps evolved at high strains are represented in Fig. 6. These micrographs show slightly elongated (sub)grains with boundaries of moderate to high misorientation angles. Based on the detailed analysis of Fig. 6(a), the misorientation angles for most of the longitudinal boundaries are higher than those for the transverse ones. The misorientation for the latters is commonly below 15°. The most of submicron scale grains formed at $\varepsilon = 8$, contains relatively low density of dislocation in their interiors, and have rather neat and smooth boundaries. It can be seen in Fig. 6(b), that an increase in the strain to $\varepsilon = 12$ is accompanied by fully development of fine grains surrounded by HABs with more recovered interiors by comparing with those evolved at $\varepsilon = 8$.

Fig. 7 represents changes in the average crystallite sizes in parallel and transverse directions to the elongated (sub)grain structure as well as the spacing of DBs with repeated ECAP at 250 °C. It is interesting to note that the spacing of DBs and the longitudinal (sub)grain size, which are derived from the data of OIM and TEM, rapidly decrease with deformation to $\varepsilon = 4$ and the both approach transverse grain size value in high strain interval, i.e. $6 \leq \varepsilon \leq 12$. Pressing to a final strain of 12 results in a full formation of roughly equiaxed grains with an average size of about 1.2 μm. In other words, the (sub)grain size at high strains is roughly equal to the spacing of DBs within some experimental scatters. This suggests that the crystallite size evolved during ECAP may be controlled by the density of DBs and thus main mechanism of grain refinement operating in the present Al alloy can be directly associated with grain fragmentation due to formation of high density DBs.

3.4. Misorientation distribution

Fig. 8 shows the misorientation distributions of the deformation-induced boundaries developed during repeated ECAP. The distributions at low-to-moderate strain, are mainly characterized by a single peak at around low angles. The misorientation distributions developed at $\varepsilon = 1$ and 2 are almost similar and the average value does not exceed 5° due to formation of high density dislocation substructures (Fig. 8(a)). The DBs and fine (sub)grains, which start to form frequently at strain of about 3, result in development of a large number of HABs with misorientation above 15°. In Fig. 8(b), the misorientation distribution at $\varepsilon = 3$, is shifted to higher angles. With further ECAP, the fraction of LABs rapidly decreases and that of HABs contrary rises at strains of 4 and 6 (Fig. 8(c) and (d)). A bimodal misorienta-

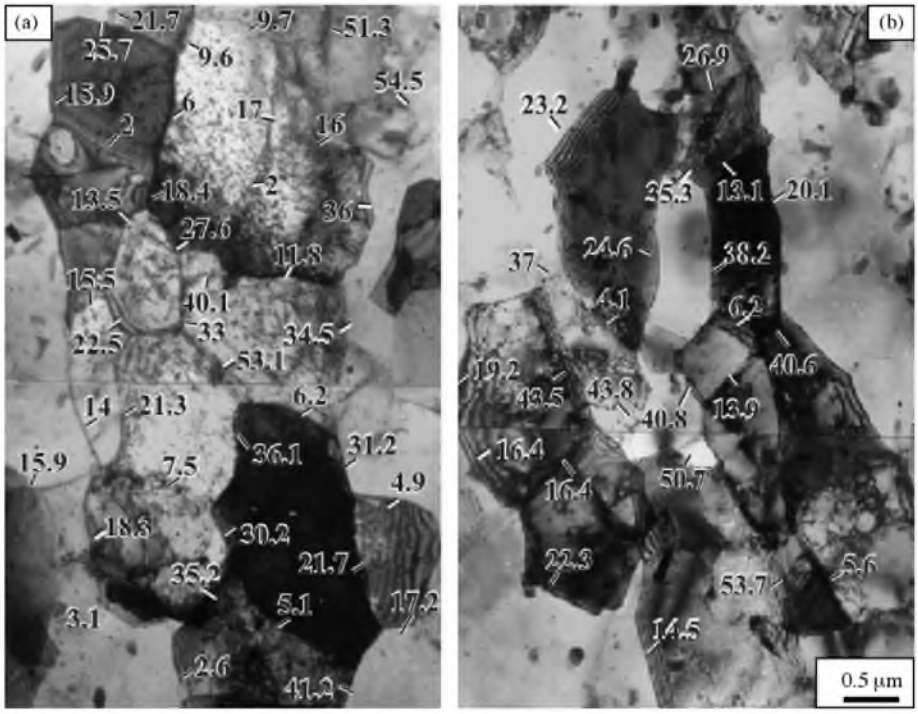

Fig. 6. TEM microstructures with misorientation maps of 2219 Al alloy deformed by ECAP at 250 °C. The numbers indicate misorientation angle in degrees. (a) $\varepsilon = 8$ and (b) $\varepsilon = 12$.

tion distribution with two peaks at low and high misorientations is developed at high strains above 6 (Fig. 8(d)–(f)). The distribution developed at $\varepsilon = 12$ is roughly similar to a random one for annealed cubic metals [20], as indicated by dashed line in Fig. 8(f). At the same time, the fraction of LABs is relatively high at $\varepsilon = 12$, that is a characteristic of a deformation-induced microstructure [20].

The effect of ECAP on the average misorientation (Θ_{av}), the fractions of HABs (F_{HAB}) and strain-induced new grains (V_{rex}) with repeated ECAP, are summarized in Fig. 9. The data derived from EBSP and TEM are roughly similar within the experimental scatters at low strains below $\varepsilon = 3$, while the values obtained from TEM are always higher than those measured by EBSP in high strain interval. This may occur because the TEM data were obtained by Kikuchi-line technique in rather small areas compared to the statistical OIM results in wider areas. It is seen in Fig. 9(a) that Θ_{av} increases to about 5° and shows a plateau at low strains of $\varepsilon \leq 2$, i.e. the strain-induced boundaries evolved in this interval are almost low ones. The average misorientation starts to grow at a strain above 2 and increases continuously with repeated ECAP to $\varepsilon = 6$ approaching gradually a saturation value of $\Theta_{av} = 32°$ at high strain. Changes in the fraction of HABs with deformation are also similar to those in the Θ_{av} (Fig. 9(b)). Namely, strain-induced HABs are scarcely developed at $\varepsilon < 2$ and then the F_{HAB} starts to increase and approaches a saturation value of about 80%. It should be noted in Fig. 9(b) that the fraction of strain-induced new grains changes roughly similar to that of high angle boundaries. Deformation by ECAP to final strain of 12 resulted in the development of new fine grains with fraction of about 90% in a whole material.

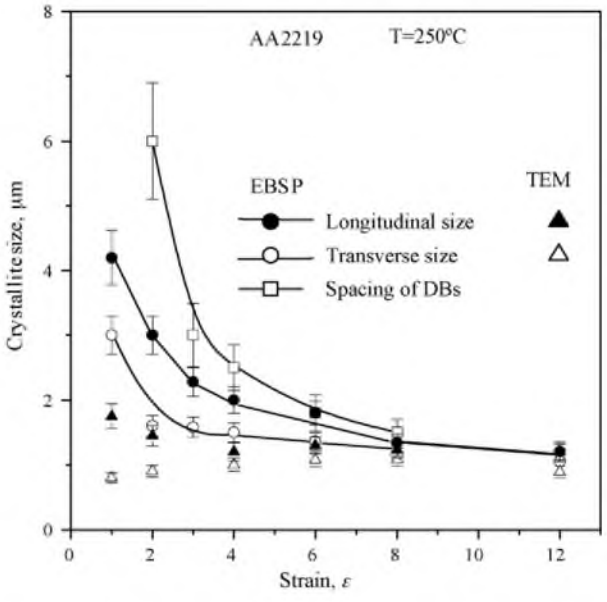

Fig. 7. Changes of the average crystallite size and spacing of deformation bands with repeated ECAP for 2219 Al alloy.

4. Discussion

4.1. New grain formation process during ECAP

The microstructure changes in a coarse grained 2219 Al alloy during ECAP to a strain of 12 at 250 °C was studied in the present work and the main features of this process can be summarized as follows:

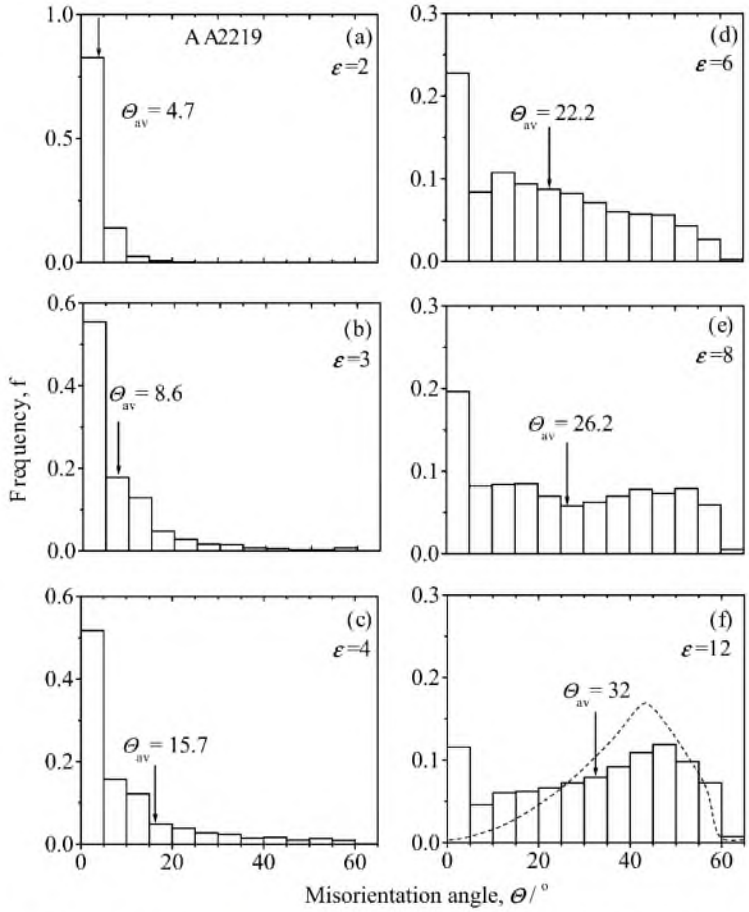

Fig. 8. Changes in the misorientation distribution of deformation-induced boundaries with repeated ECAP for 2219 Al alloy at 250 °C. The broken line indicates the random misorientation distribution for annealed materials [20].

(1) In early stages of deformation, i.e. at $\varepsilon \leq 2$, high density dislocation substructures with misorientation angles less than 5° are homogeneously developed in original grain interiors accompanied by numerous boundaries with low-to-moderate misorientation angles appearing as embryos of deformation bands. These DBs formed roughly parallel to PD and contain elongated subgrains with misorientation angles of $5^\circ \leq \Theta \leq 15^\circ$, while conventional equiaxed subgrains with LABs of $\Theta \leq 5^\circ$ are developed in the exteriors of DBs.
(2) The number and the average misorientation of DBs increase with further deformation by ECAP, leading to fragmentation of original coarse grains into different orientation regions and finally to a full development of fine grains at high strains. New grains surrounded by HABs are formed firstly in the regions of DB interiors at $\varepsilon = 3$ and subsequently the exteriors at medium to high strains.
(3) The evolved new grains are reoriented and progressively randomized with repeated ECAP at 250 °C.

Let us discuss the main factors promoting the formation of DBs as well as new fine grains. It is shown in [8,9,14–18,20] that DBs with a persistent nature, such as microshear and kink bands, can be developed by strain heterogeneity taking place due to compatibility requirements of neighboring grains or any intrinsic instability of grain during plastic deformation [20]. Formation of DBs can be strongly dependent on deformation mode and deformation conditions as well as material compositions, texture and the initial microstructure of materials. At elevated temperatures, dynamic recovery and grain boundary sliding are frequently operating and so can generally result in hard development of DBs through relaxation of strain heterogeneity [18–21]. The present 2219 Al alloy, however, contains high density of secondary precipitates of the θ phase and some dispersoids of transition metals, such as Al_3Cr, Al_3Zr and Al_6Mn, which are distributed inhomogeneously in the material (see Figs. 1, 5 and 6). These can play an important role for retardation of dislocation rearrangement and stabilization of strain-induced boundaries during repeated ECAP, leading to retardation or prevention of any relaxation of strain gradient developed in grain interiors. DBs can be developed under such severe deformation conditions. Moreover, it has been pointed in [9,16,18] that inhomogeneous deformation characteristics of ECAP can lead to the formation of DBs due to accommodation of strain gradients evolved by ECAP. Repeated ECAP can also introduce DBs in different directions and so results in mutual crossing of DBs [9,16–18].

From the present results, the microstructural changes in a strain interval from 2 to 4 are mainly characterized by frequent development of DBs as well as usual dislocation subgrains with LABs (Figs. 1–5). DBs with moderate angle are continuously

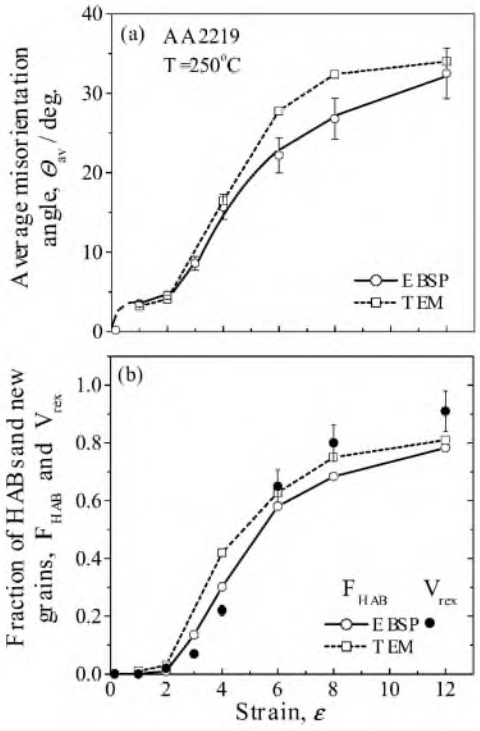

Fig. 9. Changes in (a) average misorientation angle Θ_{av}, and (b) the fraction of strain-induced HABs F_{HAB} as well as new grains V_{rex} with repeated ECAP at 250 °C for AA2219.

formed with increasing the strain from 2 to 3, so that the density of DBs rapidly grow, leading to initial grain fragmentation into different misoriented regions. In such a way, the regions which contain high density of DBs may be much more favorable sites for new grain formation, compare to the other areas with conventional subgrain structure with LABs. This may be supported by the data presented in Fig. 7, which shows that the spacing of DBs becomes roughly equal to the average crystallite size developed in high strain. Such strain-induced grains are easily evolved near and along initial grain boundaries, where high density DBs was introduced by severe plastic deformation. It is concluded, therefore, that development process of new fine grains can be a series of deformation-induced continuous reactions, that is similar to cDRX [8,9,16–18].

4.2. *Mechanism of strain-induced grain refinement*

A process of development of deformation-induced boundaries during repeated ECAP is schematically represented in Fig. 10. Changes in the average misorientation angle Θ_{av} with deformation can be subdivided into three different stages, denoted as stages 1, 2 and 3 in Fig. 10. The Θ_{av} increases to a plateau of about 5° at the initial stage of 1, then rapidly increases in stage 2 and finally approaches a saturation high value in stage 3. A small increasing of the Θ_{av} in stage 1 is related to homogeneous formation of usual dislocation substructures with LABs (Figs. 2 and 5(a)), which do not change significantly until a critical strain ε_c [17,21]. It is interesting to note that this strain interval may correspond to a conventional "steady state" flow appearing in many commercial Al alloys under warm or

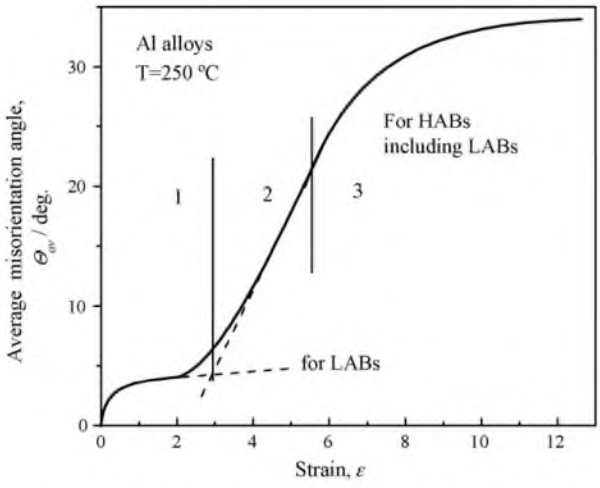

Fig. 10. Schematic drawing of the relationship between the average misorientation angle Θ_{av} of strain-induced low and high angle boundaries (LABs and HABs) and strain during severe plastic deformation in Al alloys at 250 °C.

hot deformation conditions [20,22]. It was noted, that embryos of DBs with low-to-moderate angle misorientations are introduced in the present alloy in stage 1. An increase in the strain to around ε_c, results in transformation of mentioned above embryos into macroscopic scale DBs with moderate angle misorientation. Thus, the ε_c can be considered as a macroscopic indication for evolution of the boundaries of DBs as well as the formation of strain-induced new grains [17]. Therefore, stage 1 may correspond to a kind of incubation period for new grain formation. In the following stage 2, a rapid increasing of the Θ_{av} can result from transformation of embryos of DBs into macroscopic DBs with HABs and also development of strain-induced new grains (Fig. 9). In stage 3, a gradual increasing of Θ_{av} takes place due to formation of fine grained structure with HABs developed in the whole material.

It is concluded, therefore, that significant increasing of the average misorientation angle in stage 2 is resulted mainly from frequent evolution of DBs, followed by full formation of a new grain structure in stage 3. It is interesting to note, that similar results on the process of strain-induced grain formation during SPD are reported in several recent papers [8,16,21], in which a 7475 Al alloy was severely deformed not only by ECAP, but also by multi-directional forging (MDF). It was found, that the operation of grain boundary sliding takes place in new fine grained regions in 7475 Al alloy deformed by MDF at 250 °C [21]. Under such deformation conditions, frequent grain boundary sliding is accompanied by grain rotation, leading to randomization of the crystal orientation of each newly evolved grain [8], as shown in Figs. 3 and 4 for the present 2219 Al alloy.

5. Conclusions

The microstructure evolution in a coarse grained 2219 aluminum alloy during ECAP to strains of 12 at 250 °C was studied in the present work. The main results are summarized as follows:

(a) The process of microstructural changes during ECAP can be subdivided into three stages: i.e. an incubation period for new grain evolution in stage 1; grain fragmentation by frequent formation of DBs in stage 2 and full development of new fine grains in stage 3.
(b) In stage 1, below a critical strain, conventional dislocation substructures with LABs are homogeneously developed accompanied by embryos of DBs.
(c) In stage 2, such embryos can transform into macroscopic DBs. The number and the average misorientation of the boundaries of DBs rapidly grow with increasing the deformation, leading to original grain fragmentation into different misoriented regions.
(d) In stage 3, new grains surrounded by HABs are fully developed in a whole material accompanied by randomization of the crystal orientations at high strains.
(e) It is concluded, therefore, that process of new grain formation can be a series of deformation-induced continuous reactions, that is cDRX.

Acknowledgments

The authors acknowledge with gratitude the financial supports received from Ministry of Education, Science and Culture and Light Metals Education Foundation in Japan. One of the authors (I.M.) would like to express hearty thanks to the Japanese government for providing the scholarship.

References

[1] R.Z. Valiev, R.K. Islamgaliev, I.V. Alexandrov, Prog. Mater. Sci. 45 (2000) 103–189.
[2] V.M. Segal, Mater. Sci. Eng. A 386 (2004) 269–276.
[3] M. Furukawa, Z. Horita, M. Nemoto, T.G. Langdon, Acta Mater. 45 (1997) 4733–4741.
[4] Y. Iwahashi, Z. Horita, M. Nemoto, T.G. Langdon, Acta Mater. 46 (1998) 3317–3331.
[5] R.Z. Valiev, T.G. Langdon, Prog. Mater. Sci. 51 (2006) 881–981.
[6] A. Gholinia, F.J. Humphreys, P.B. Prangnell, Acta Mater. 50 (2002) 4461–4476.
[7] A. Gholinia, P.B. Prangnell, M.V. Markushev, Acta Mater. 48 (2000) 1115–1130.
[8] O. Sitdikov, T. Sakai, A. Goloborodko, H. Miura, R. Kaibyshev, Phil. Mag. 85 (2005) 1159–1175.
[9] A. Goloborodko, O. Sitdikov, T. Sakai, R. Kaibyshev, H. Miura, Mater. Trans. 44 (2003) 766–774.
[10] C. Xu, M. Furukawa, Z. Horita, T.G. Langdon, Mater. Sci. Eng. A 398 (2005) 66–76.
[11] S. Gourdet, F. Montheillet, Mater. Sci. Eng. A 283 (2000) 274–288.
[12] H.J. McQueen, Mater. Sci. Eng. A 387–389 (2004) 203–208.
[13] M.E. Kassner, S.R. Barrabes, Mater. Sci. Eng. A 410–411 (2005) 152–155.
[14] O. Sitdikov, T. Sakai, A. Goloborodko, H. Miura, Scripta Mater. 51 (2004) 175–179.
[15] X. Yang, H. Miura, T. Sakai, Mater. Trans. 44 (2003) 197–203.
[16] A. Goloborodko, O. Sitdikov, R. Kaibyshev, H. Miura, T. Sakai, Mater. Sci. Eng. A 381 (2004) 121–128.
[17] T. Sakai, in: Y.T. Zhu, T.G. Langdon, Z. Horita, M.J. Zehetbauer, S.L. Semiatin, T.C. Lowe (Eds.), Ultrafine Grained Materials IV, vol. 237, TMS, 2006, pp. 73–80.
[18] O. Sitdikov, T. Sakai, E. Avtokratova, R. Kaibyshev, Y. Kimura, K. Tsuzaki, Mater. Sci. Eng. A 444 (2007) 18–30.
[19] O. Sitdikov, R.O. Kaibyshev, I.M. Safarov, I.A. Mazurina, Phys. Met. Metallogr. 92 (2001) 270–280.
[20] F.J. Humphreys, M. Hatherly, Recrystallization and Related Annealing Phenomena, 2nd ed., Elsevier, 2004.
[21] A. Goloborodko, T. Sakai, O. Sitdikov, H. Miura, Mater. Sci. Forum 539–543 (2007) 2922–2927.
[22] J. Gil Sevillano, P. vanHoutte, E. Aernoudt, Prog. Mater. Sci. 25 (1980) 69–412.